Theoretical and Applied Climatology (2019) 136:915–928
https://doi.org/10.1007/s00704-018-2527-0

ORIGINAL PAPER

# Characteristics of vegetation activity and its responses to climate change in desert/grassland biome transition zones in the last 30 years based on GIMMS3g

Jing Hou[1] · Lingtong Du[1] · Ke Liu[1] · Yue Hu[1] · Yuguo Zhu[1]

Received: 9 March 2017 / Accepted: 28 May 2018 / Published online: 2 June 2018



## Abstract

The vegetation in desert/grassland biome transition zones is part of a fragile ecosystem that is sensitive to climate change. Thus, in recent decades, studying vegetation activity in desert/grassland biome transition zones has become important. Here, vegetation activity and the evolutionary tendencies of the temporal and spatial differentiation of the phenology of the desert/grassland biome transition zones were analyzed based on the Normalized Difference Vegetation Index (NDVI) of the third-generation Global Inventory Modeling and Mapping Studies (GIMMS3g) dataset. Additionally, the relationship between vegetation activity and climatic factors was analyzed based on NDVI and global meteorological reanalysis data. The results showed that the vegetation phenology of desert/grassland biome transition zones exhibits sharply contrasting characteristics between the Northern and Southern hemispheres, particularly when comparing differences before and after the breakpoint in global climate change (1998). The length of the growing season (LOS) of the Northern Hemisphere was shorter after 1998 than before it, and the integral of the growing season (IOS) of the NDVI decreased correspondingly. By contrast, the LOS in the Southern Hemisphere was longer, and after 1998, the IOS of the NDVI increased compared to its previous value. The vegetation activity trend and the fluctuation of the desert/grassland biome transition zones in the last 30 years can be divided into nine combined modes. However, these features also have an obvious turning point in 1998. The effects of evapotranspiration and precipitation on vegetation activity were most obvious, and these climatic factors drove the phenology changes in the different regions. Global warming limited the vegetation activity in low-latitude areas, but promoted it in middle-latitude areas.


## 1 Introduction

Climate is an important determinant of land surface characteristics such as biome distributions and vegetation phenology, especially in arid and semi-arid areas (Weiss et al. 2004). As a key component of the terrestrial ecosystem, vegetation plays a key role in the interactions between the atmosphere and land surface. In recent years, the response of vegetation to climate change has become an active research field because inter-annual and seasonal variations in vegetation can be a sensitive indicator of global climate change (Qian et al. 2010). The Normalized Difference Vegetation Index (NDVI) is an important parameter that reflects changes in vegetation cover and its growth status (Myneni et al. 1997). Long-term NDVI data can be used to monitor the characteristics of annual growth, phenology changes, spatial evolution, and drought impacts on vegetation and reflects the response of vegetation activity to climate change by using the relationship between the NDVI and climatic factors (Bao et al. 2015; Du et al. 2013, 2017; Martínez and Gilabert 2009; Rogier et al. 2011). Statistical methods have been developed and applied to NDVI time series to detect the overall trend, slope, and inter-annual variability in the fields of ecosystem productivity and natural disasters (Forkel et al. 2013; Huang et al. 2013). This research has motivated scientists to use the inter-annual variability of NDVI to monitor the ecosystem response to climate change at global scales (Zeng et al. 2013). Fensholt et al. (2012) reported that the NDVI of global semi-arid regions increased by an

✉ Lingtong Du
dult80@qq.com

[1] Breeding Base for State Key Laboratory of Land Degradation and Ecological Restoration in Northwest China, Key Laboratory for Restoration and Reconstruction of Degraded Ecosystem in Northwest China of Ministry of Education, Ningxia University, No.489 Hanlanshan Road, Yinchuan 750021, China

average of 0.015 from 1981 to 2007. Analysis of the status of vegetation growth in high-latitude areas in the Northern Hemisphere based on Global Inventory Modeling and Mapping Studies (GIMMS) data has shown that rising temperature is closely correlated with the increase in NDVI (Slayback et al. 2010). The changes in phenology exhibited a pronounced latitudinal zonality in the Northern Hemisphere, with the start of growing season (SOS) being advanced significantly in high-latitude areas and, from 1982 to 2006, the end of growing season (EOS) being more obviously in mid-latitude areas (Jeganathan et al. 2014). Differences in sensitivity to climate change are due to different vegetation types and ecosystems (Bunn et al. 2007; Scholze et al. 2006). Therefore, an analysis of the vegetation of climate-sensitive areas promotes the understanding of global climate change.

The desert/grassland biome transition zone lies between the desert and grassland and is characterized by arid and semi-arid climate, rare precipitation, sparse vegetation, low biodiversity, and harsh and fragile natural conditions and resources. The geographic location of the desert/grassland biome transition is primarily determined by climatic factors (Kröel-Dulay et al. 2004). Thus, the fluctuations or directional changes in climate are expected to have large effects on these areas, such as a shift in the status of vegetation growth and phenology (Kröel-Dulay et al. 2004). Therefore, in the context of global climate change, a study of vegetation activity and responses to climatic factors in desert/grassland biome transition zones can be expected to contribute to exploring the mechanisms of precipitation and temperature redistribution as they pertain to vegetation growth. Due to their arid climate, sparse vegetation, and fragile ecosystem, desert/grassland biome transition zones are easily influenced by climate change and are thus more sensitive to it than are other terrestrial ecosystems (Bao et al. 2016; Chen et al. 2017a, b; Hochstrasser et al. 2002). At different temporal scales, the study of vegetation responses to climate in desert/grassland biome transition zones can be used to understand and simulate dynamic changes in the terrestrial ecosystem, as well as reveal the features of global climate change.

Different kinds of long-term time series NDVI datasets that derive from Advanced Very High Resolution Radiometer (AVHRR), Satellite Pour l'Observation de la Terre Vegetation (SPOT-VGT), and Moderate Resolution Imaging Spectroradiometer (MODIS) have been published over the past decades. There are also several AVHRR-derived NDVI datasets with different corrections for sensor and atmospheric effects (Beck et al. 2011). Among them, the third-generation GIMMS NDVI dataset (GIMMS3g) is the longest global submonthly time series of NDVI available and has been crucial to studying a variety of global land vegetation processes from 1981 to 2012 (Anyamba et al. 2014; Campo-Bescós et al. 2013; Pinzon and Tucker 2014). New features of this dataset include reduced NDVI variations arising from calibration, view geometry, volcanic aerosols, and other effects not related to actual vegetation activity (Pinzon and Tucker 2014). Therefore, compared to other remote sensing products, the GIMMS3g has obvious advantages in vegetation monitoring at large spatiotemporal scales. In this study, spatiotemporal changes in vegetation growth and phenology in the global desert/grassland biome transition zones over the last 30 years were analyzed. Climatic factors driving phenology change as well as the response mechanism of the vegetation to climate change in different spatiotemporal scales were also analyzed by coupling global meteorological reanalysis data. Thus, this study provides a scientific basis and support for improving the ecological environment of the desert/grassland biome transition zones and predicting the impact of future global climatic changes on terrestrial ecosystems.

## 2 Data and methods

### 2.1 Remote sensing and meteorological data

Derived from the NOAA's AVHRR for the period 1982–2012 with a 15-day temporal frequency, the GIMMS3g NDVI data have been crucial to studying ecological processes on continental and global scales (Pinzon and Tucker 2014). With the rapid advancement in meteorological data assimilation technology, historical climate datasets with high spatial–temporal resolution have been reconstructed by some institutions (Laloyaux et al. 2016). Here, precipitation data were obtained from the NOAA's land precipitation data (PREC/L) with this historical reconstruction (Chen et al. 1997), surface temperature data were obtained from the Global Historical Climatology Network's Climate Anomaly Monitoring System (GHCN-CAMS) (Fan and Dool 2008), monthly evapotranspiration and photosynthetically active radiation data at the surface were obtained from the ERA-Interim atmospheric reanalysis system of the European Centre for Medium-range Weather Forecast (ECMWF) (Dee et al. 2011; Uppala et al. 2005), and daily surface temperature data were obtained from the JRA-55 data of the Japan Meteorological Agency (Ebita et al. 2011; Kobayashi et al. 2015). In addition, global land cover data were used from GlobCover (Tchuenté et al. 2011). All meteorological data were resampled into a spatial resolution of 8 km consistent with the resolution of NDVI (Table 1).

### 2.2 Extraction of desert/grassland biome transition zone

The desert/grassland biome transition zone, not a typical terrestrial biome, is part of the classification of grassland types (Ren 2008) and considers multiple factors such as temperature, precipitation, and land cover. At the global scale, the lower vegetation cover grassland and shrub area with arid

**Table 1** Survey of remote sensing and meteorological data

| Datasets | Index | Spatial resolution | Temporal resolution |
|---|---|---|---|
| GIMMS3g | NDVI | 8 × 8 km | 15 days |
| PREC/L | Precipitation | 0.5 × 0.5° | Monthly |
| GHCN-CAMS | Temperature | 0.5 × 0.5° | Monthly |
| ERA-Interim | Evapotranspiration | 0.75 × 0.75° | Monthly |
| | Photosynthetically active radiation | 0.75 × 0.75° | Monthly |
| Jra-55 | Air temperature | 1.25 × 1.25° | Monthly |
| GlobCover | Land cover type | 300 × 300 m | |

climate conditions are defined as the desert/grassland biome transition zone. Here, the spatial climate data and global land cover data were assembled in a Geographic Information System (GIS) software to extract the desert/grassland biome transition zone. This zone is characterized by annual precipitation between 100 and 400 mm, daily average atmospheric temperature higher than 0 °C, accumulated temperature higher than 2300 °C, and wet coefficient between 0.3 and 1.3. The wet coefficient was calculated from the PREC/L precipitation and the JRA-55 annual accumulated temperature. Fragmented areas of the extracted desert/grassland biome transition zones were eliminated, and nine partitions are obtained at the worldwide scale (Fig. 1).

## 2.3 Methods

1. Trend analysis. To explore the trend of vegetation growth indicators, the relationships between vegetation growth indicators ($\hat{y}_i$ ) and time ($t_i$) were simulated using a linear regression algorithm. The slope of the regression was calculated pixel by pixel through the least squares method, and the *F*-test was used to examine the level of significance of the regression. The linear regression equation was defined by the following formula:

$$\hat{y}_i = a + bt_i \tag{1}$$

The regression coefficient $b$ has the following expression:

$$b = \frac{n \times \sum_{i=1}^{n} (t_i \times y_i) - \sum_{i=1}^{n} t_i \sum_{i=1}^{n} y_i}{n \times \sum_{i=1}^{n} t_i^2 - \left(\sum_{i=1}^{n} t_i\right)^2} \tag{2}$$

2. Fluctuation analysis. The time series of NDVI data consisted of a linear trend and fluctuation. The linear trend could be simulated by linear regression. To eliminate the disturbance of the small periodic vibration, a moving average series ($y_i$') of the original NDVI series was obtained. The residual of the moving average NDVI and the simulated linear trend were defined as the fluctuation component, and its absolute value $z_i$ was calculated using the following formula:

$$z_i = \left| y_i' - a - bt_i \right| \tag{3}$$

To detect the characteristics of the fluctuation, a least squares method was used to establish a linear regression equation of $z_i$ and the corresponding time $t_i$.

$$\hat{z}_i = c + dt_i \tag{4}$$

The regression coefficient $d$ represents the eigenvalues of the fluctuation characteristics of the original NDVI series. A value of $d$ greater than 0 indicates that $z$ increases with time, that is, the fluctuation of variables is enhancing; $d$ less than 0 means that $z$ decreases with time, that is, the fluctuation of variables is weakening. The magnitude of $d$ reflects the magnitude of the fluctuation (Shi et al. 2014). Based on the characteristics of the linear trend and fluctuation, vegetation activity was divided into nine modes (Fig. 2).

3. Correlation analysis. The Pearson correlation coefficient of the vegetation indicator in each desert/grassland biome transition zone was calculated to explore the relationships of vegetation activity in each region:

$$r_{xy} = \frac{\sum_{i=1}^{n} \left(x_i - \overline{x}\right)\left(y_i - \overline{y}\right)}{\sqrt{\sum_{i=1}^{n} \left(x_i - \overline{x}\right)^2 \sum_{i=1}^{n} \left(y_i - \overline{y}\right)^2}} \tag{5}$$

where $r_{xy}$ is the correlation coefficient, $x_i$ and $y_i$ represent annual NDVI in different regions, $\overline{x}$ and $\overline{y}$ are the means of annual NDVI in different regions during the study period, and $n$ is the length of time segments.

Partial correlations among vegetation and precipitation, temperature, evaporation, and photosynthetically active radiation were established to explore the relationship between vegetation activity and climate factors:

$$r_{xy,z} = \frac{r_{xy} - r_{xz} r_{yz}}{\sqrt{\left(1 - r_{xz}^2\right)\left(1 - r_{yz}^2\right)}} \tag{6}$$

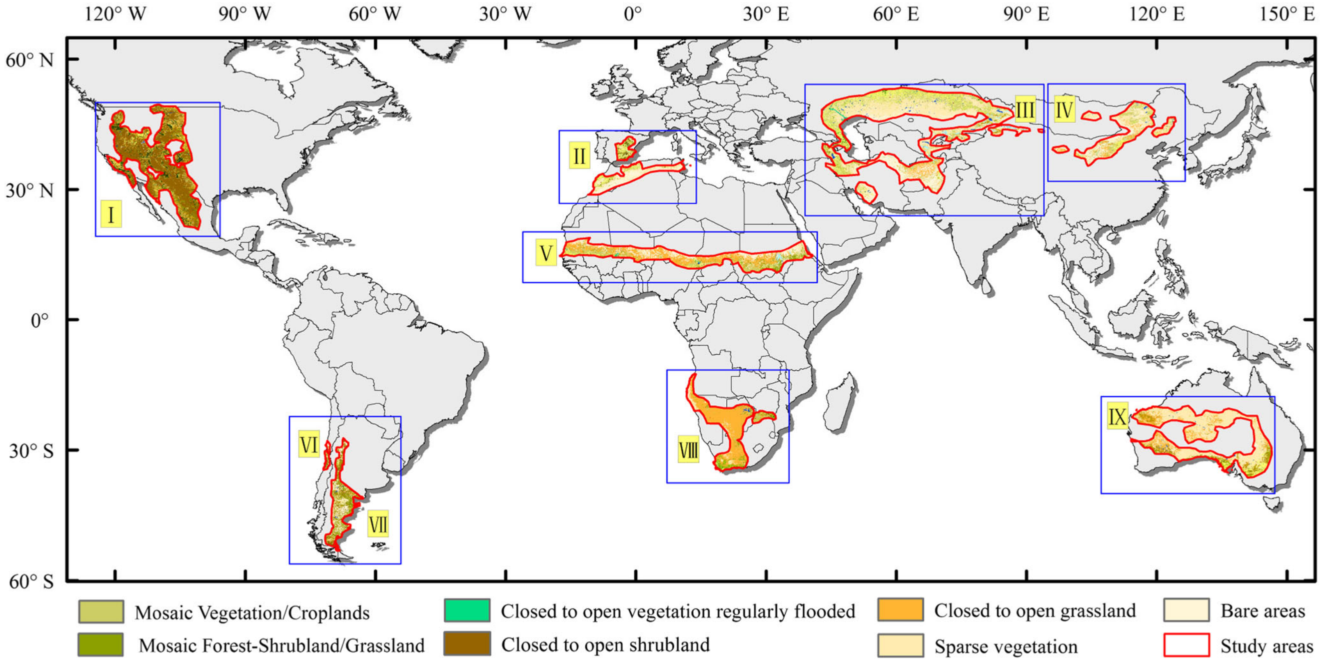


**Fig. 1** Distribution of desert/grassland biome transition zones. Nine partitions are (I) North American, (II) Mediterranean Coast, (III) Central Asia, (IV) East Asia, (V) Sahel Region, (VI) Mediterranean climate region of South American West Coast, (VII) East Coast of South America, (VIII) South Africa, and (IX) Australia

where $r_{xy,z}$ is the partial correlation coefficient between the vegetation index ($x$) and a meteorological factor ($y$), with other climatic factors ($z$) as controlling conditions.

4. Phenology estimation. To reveal the phenology change of the desert/grassland biome transition zone in recent decades, the NDVI time series have been reconstructed and used to estimate their phenology characteristics. Due to the influence of aerosol, the performance of the sensor, the angle of sunlight, and surface water, the long time series of vegetation activity observed was usually indented with irregular fluctuations, and a seasonal variation trend was not obvious. Therefore, the asymmetric Gaussian (AG) function was used to gradually fit the vegetation growth curve, and the reconstructed NDVI series was achieved by smoothing the Gaussian fitting curve. At the same time, the characteristic parameters of the growth seasons were defined using the software Timesat (Jönsson and Eklundh 2004). The SOS and EOS were estimated as 30% of the rising and falling curve, respectively. The time between SOS and EOS was defined as the length of growing season (LOS) and the integral value of the LOS curve was defined as the integral of growing season (IOS), which reflected the total ground vegetation (Fig. 3).

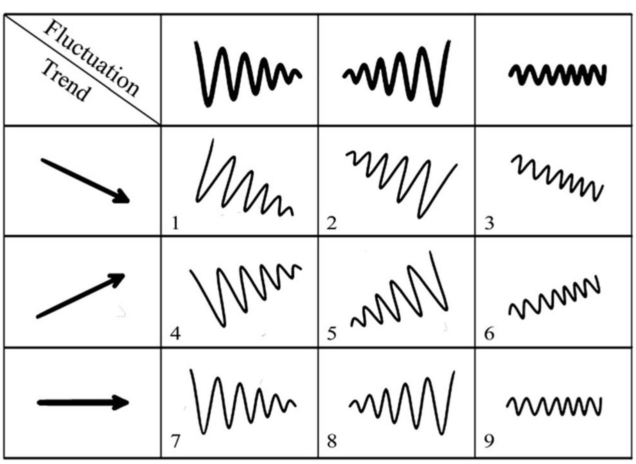


**Fig. 2** Modes of vegetation activity. Nine modes are (1) decreasing trend and weakening fluctuation, (2) decreasing trend and enhancing fluctuation, (3) decreasing trend and stable fluctuation, (4) increasing trend and weakening fluctuation, (5) increasing trend and enhancing fluctuation, (6) increasing trend and stable fluctuation, (7) no trend and weakening fluctuation, (8) no trend and enhancing fluctuation, and (9) no trend and stable fluctuation

## 3 Results and analysis

### 3.1 Basic characteristics of vegetation activity

#### 3.1.1 Spatial distribution of NDVI and analysis of regional correlation

The annual average NDVI values are between 0.2 and 0.4 in global desert/steppe transition zones because the vegetation is sparse. The spatial distribution of NDVI in the nine partitions

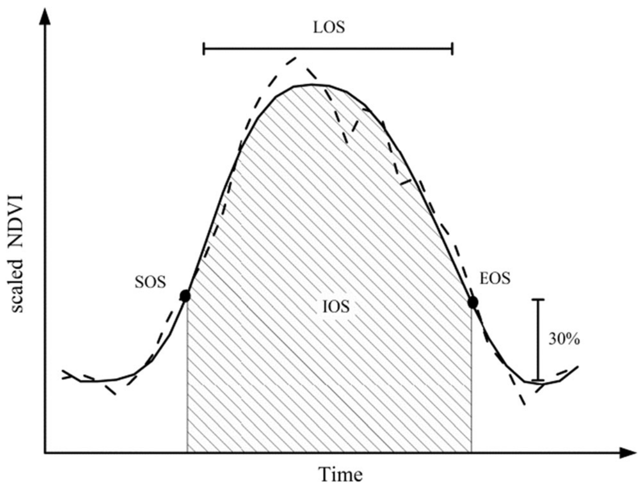


**Fig. 3** Definition of phenology parameters. SOS is the start of growing season, EOS is the end of growing season, LOS is the length of growing season, and IOS is the integral of growing season. The dashed curve is the original NDVI series and solid curve is the reconstructed NDVI series

is shown in Fig. 4. More detailed information was obtained from the annual average NDVI in each region: (1) The mean value of NDVI in the Mediterranean climatic region of the South American West Coast (Fig. 4(VI)) is 0.38, the highest globally and significantly higher than that of the East Coast of South America (Fig. 4(VII)) even though they are geographically proximate. The next is the North America, with a mean NDVI value of 0.31 (Fig. 4(I)). The partitions with relatively low NDVI values are the East Asia (Fig. 4(III)), Central Asia (Fig. 4(IV)), the Sahel Region (Fig. 4(V)), and the Mediterranean Coast (Fig. 4(II)), with mean NDVI values of 0.22, 0.23, 0.22, and 0.25, respectively, because all these four partitions have an obvious desert region. However, the mean values of the NDVI in South Africa (Fig. 4(VIII)) and Australia (Fig. 4(IX)) are 0.29 and 0.28, respectively. (2) The spatial distributions of NDVI in the Mediterranean Coast (Fig. 4(II)), East Asia (Fig. 4(III)), and Central Asia (Fig. 4(IV)) have the same pattern, in that the NDVI in the northern regions was generally higher than that of the southern regions. However, the spatial characteristics of NDVI in the Sahel Region (Fig. 4(V)) are opposite, in that it showed high values in the southern areas and low ones in the northern, because this partition is near the Equator. The NDVI in North America (Fig. 4(I)) is highly spatially heterogeneous and distinct from the spatial distributions of NDVI in South Africa and Australia (Fig. 4(VIII), (IX)).

A correlation analysis of NDVI in global desert/steppe transition zones (Table 2) indicates that moderate positive correlations are found in the same latitude of the same

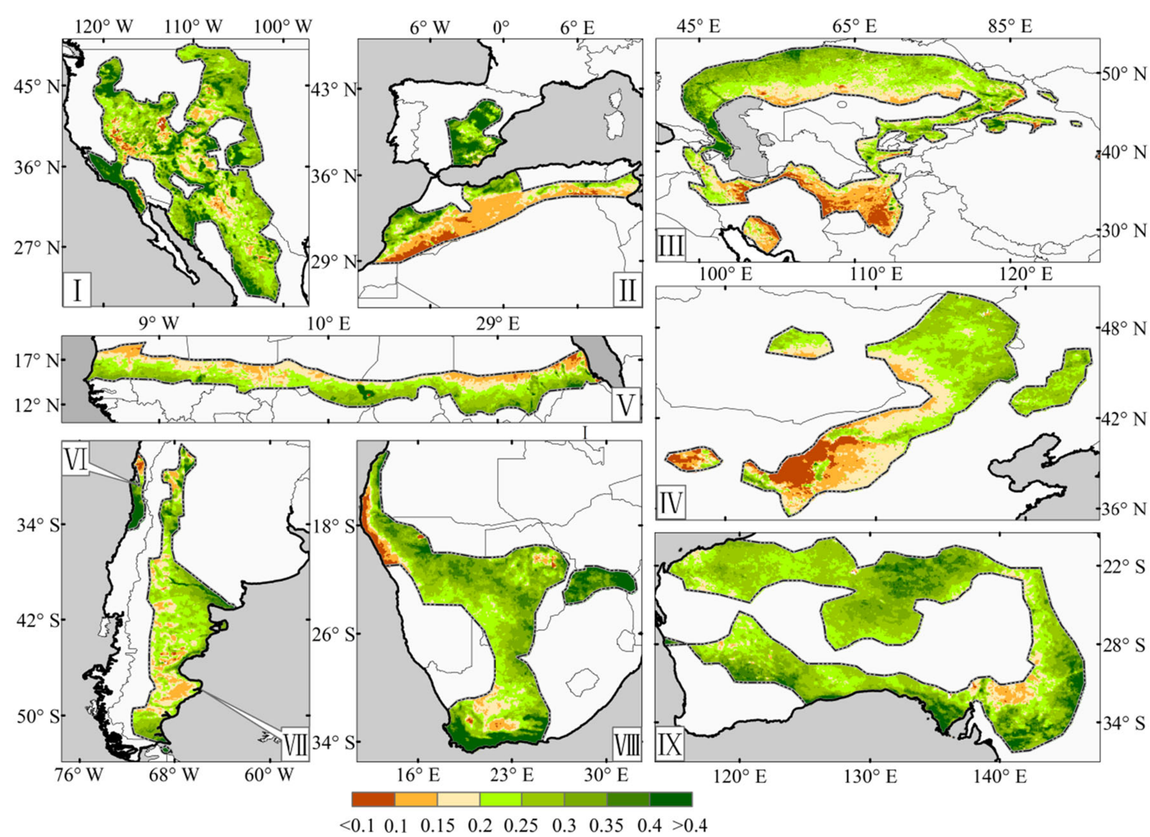


**Fig. 4** Spatial distribution of annual NDVI in desert/grassland biome transition zones. Nine partitions are (I) North American, (II) Mediterranean Coast, (III) Central Asia, (IV) East Asia, (V) Sahel Region, (VI) Mediterranean climate region of South American West Coast, (VII) East Coast of South America, (VIII) South Africa, and (IX) Australia

**Table 2** Correlation matrix of annual NDVI of each desert/grassland biome transition zone

| | I. North American | II. Mediterranean Coast | III. Central Asia | IV. East Asia | V. Sahel Region | VI. Mediterranean climate region of South America West Coast | VII. East Coast of South America | VIII. South Africa | IX. Australia |
|---|---|---|---|---|---|---|---|---|---|
| I. North American | 1.000 | 0.291 | 0.398* | 0.055 | −0.131 | 0.017 | −0.261 | 0.098 | 0.099 |
| II. Mediterranean Coast | | 1.000 | 0.163 | 0.427* | −0.024 | −0.201 | −0.545** | 0.455* | 0.384* |
| III. Central Asia | | | 1.000 | 0.252 | 0.225 | −0.033 | −0.004 | −0.032 | 0.066 |
| IV. East Asia | | | | 1.000 | 0.290 | −0.384* | −0.056 | 0.312 | 0.163 |
| V. Sahel Region | | | | | 1.000 | −0.326 | 0.324 | 0.183 | 0.015 |
| VI. Mediterranean climate region of South America West Coast | | | | | | 1.000 | 0.292 | −0.045 | 0.091 |
| VII. East Coast of South America | | | | | | | 1.000 | −0.215 | −0.324 |
| VIII. South Africa | | | | | | | | 1.000 | 0.541** |
| IX. Australia | | | | | | | | | 1.000 |

*Significant at 0.05 probability level

**Significant at 0.01 probability level

hemisphere, such as Central Asia and North America (Northern Hemisphere) and South America and Australia (Southern Hemisphere). This result indicates that although the partitions are in different continents, the NDVIs in the same latitude of the same hemisphere have the same change characteristics. The annual average NDVI in the Mediterranean Coast, which has a special geographical position and climate type, recorded a particular correlation with those of East Asia, South Africa, Australia, and the East Coast of South America. Different from the positive correlations among other regions, the annual average NDVI of the Mediterranean Coast and the East Coast of South America is significantly negatively correlated, with a correlation coefficient of −0.545 ($P < 0.01$). On both sides of the Atlantic, the "seesaw" phenomenon of vegetation activity is witnessed. The phenomenon whereby vegetation activity, which is influenced by climate, has obvious positive correlations in different regions can be considered as a result of global climate evolution. The negative correlations between regions could be due to the redistribution of heat and moisture on the two sides of the Atlantic.

### 3.1.2 Phenology characteristics and their changed rules

The characteristics of phenology not only differ greatly in the Northern and Southern hemispheres, but even for the same region, the range of the inter-annual fluctuations of phenology is also obviously significant (Table 3). The season of

**Table 3** Basic characteristics of phenology of each desert/grassland biome transition zone

| | Average SOS (DOY) | Earliest SOS (DOY) | Latest SOS (DOY) | Average LOS (days) | Shortest LOS (days) | Longest LOS (days) | Average IOS | Minimum IOS | Maximum IOS |
|---|---|---|---|---|---|---|---|---|---|
| I. North American | 111 | 89 | 129 | 202 | 175 | 221 | 5.54 | 4.94 | 6.08 |
| II. Mediterranean Coast | −6 | −32 | 23 | 187 | 156 | 212 | 4.00 | 3.55 | 4.72 |
| III. Central Asia | 98 | 90 | 106 | 196 | 179 | 212 | 4.65 | 4.28 | 5.04 |
| IV. East Asia | 126 | 119 | 133 | 167 | 156 | 179 | 4.22 | 3.95 | 4.60 |
| V. Sahel Region | 167 | 156 | 194 | 109 | 96 | 123 | 2.55 | 2.23 | 3.16 |
| VI. Mediterranean climate region of South American West Coast | 173 | 152 | 194 | 179 | 151 | 210 | 6.02 | 5.02 | 7.05 |
| VII. East Coast of South America | 11 | −22 | 50 | 223 | 205 | 242 | 3.72 | 3.34 | 4.13 |
| VIII. South Africa | 11 | −7 | 26 | 177 | 158 | 196 | 4.56 | 3.91 | 5.38 |
| IX. Australia | 69 | 38 | 119 | 188 | 159 | 208 | 4.44 | 3.58 | 6.11 |

Negative values indicate that vegetation growth season had begun in the previous year. DOY is day of year, SOS is the start of growing season, LOS is the length of growing season, and IOS is the integral of growing season vegetation growth is from May to October and the average LOS was 202, 196, and 167 days in North America, Central Asia, and East Asia, respectively. The three regions mentioned above are generally characterized by a continental or monsoon climate, with an increasing synchronization of temperature and precipitation, which facilitates the natural growth of vegetation. Because precipitation is the main limitation factor for vegetation growth, the Sahel, which is located in the transitional zone between the savannas and tropical deserts in the low latitudes of the Northern Hemisphere and has adequate warmth, has the latest SOS. The Sahel does not enter into the rainy season and the vegetation into growing season until the Intertropical Convergence Zone moves northward every summer. Additionally, the LOS in Sahel is the shortest with an average of 109 days, and the short LOS and the low NDVI result in the low IOS. The Mediterranean region is characterized by mild and rainy winters under the influence of the prevailing westerly winds, and the growing season is mainly concentrated in the winter. Hence, the growing season of the Mediterranean Coast is similar to that of other regions in the Southern Hemisphere. The vegetative period of the Mediterranean region of the South American west coast is similar to that of other regions in the Northern Hemisphere. Moreover, an analysis of a correlated matrix regarding the LOS of the nine regions over the last three decades found different degrees of positive correlations of the LOS between various regions, similar to the correlated analysis of the NDVI. The correlation coefficients between Australia and South Africa, North America and East Asia, North America and Mediterranean climate region of South American West Coast, North America and Central Asia, and Mediterranean Coast and South Africa are 0.516, 0.479, 0.528, 0.428, and 0.485, respectively, with all passing the significance test ($P < 0.01$). As a consequence of the seasonal movement of the planetary wind system and fluctuation of the rainfall season, there is a significant negative correlation in terms of LOS between the Mediterranean Coast and the Sahel, with a correlation coefficient of $-0.394$ ($P < 0.01$).

Over the past few decades, global warming has become an indisputable fact. However, some recent studies have claimed that there is an observed reduction in the surface warming trend over the period 1998 to 2012 (Stocker et al. 2013; Karl et al. 2015; Meehl et al. 2014; Trenberth and Fasullo 2013), although that remains debatable (Karl et al. 2015; Trenberth 2015). Hence, a hypothesis that vegetation activity and phenology have been changed by climate is put forward. To study the change characteristics of vegetation before and after the turning point, the slopes of the LOS and the IOS during 1982–1998 and 1998–2012 in each desert/grassland biome transition zone were calculated and their variations were contrasted (Fig. 5). The results show that, after 1998, the slope of the LOS decreased in the Northern Hemisphere, except the Sahel, and the slope of the LOS increased in the Southern Hemisphere, except the Mediterranean climatic region of the South American West Coast. After 1998, the slopes of all IOSs decreased in the Northern Hemisphere and, except for the East Coast of South America, those of the Southern Hemisphere increased. The changes in phenology had the opposite characteristics between the Northern and Southern hemispheres in global desert/grassland biome transition zones, such that, after 1998, most LOSs and IOSs decreased more significantly than before in the Northern Hemisphere, in contrast with regions in the Southern Hemisphere.

## 3.2 Change trend and fluctuation of vegetation

To study the fluctuation of vegetation during 1982–1998 (Fig. 6a) and 1998–2012 (Fig. 6b), the modes of vegetation activity were detected pixel by pixel using the method described in Section 2.3. Vegetation activity in 81% of the areas of the global desert/grassland biome transition zones shows an increasing trend; however, 47% of the areas show an enhancing fluctuation, and only 34% of the areas show a weakening fluctuation. Vegetation activity with a decreasing trend and weakening or enhancing fluctuation accounts for 10 and 8% of all the areas, respectively. Over 1982–1998, the areas of vegetation degradation are mainly concentrated in the Mediterranean climate region of the South American West Coast, the north and east of Australia, northwest of South Africa, and other small areas (Fig. 6a). The mode of vegetation activity of no trend or stable fluctuation only accounts for 1% of the all areas, which means that, over the last 30 years, a region with no vegetation change in the global desert/grassland biome transition zones is almost nonexistent. After 1998, vegetation activity began to weaken in large areas, and approximately 54% areas of the desert/grassland biome transition zones show a decreasing trend (Fig. 6b). Nevertheless, most decreasing areas of vegetation activity have an enhancing fluctuation which accounts for 35% of total areas. The above results have proven that the ecosystem of the global desert/grassland biome transition zone is extremely sensitive, and its vegetation is vulnerable to changes in the global environment.

Moreover, the trend and inter-annual fluctuation of NDVI in two stages shows an intense spatial differentiation. For example, the trend of vegetation activity in most areas of Central Asia, Sahel, and South America reversed completely. Furthermore, the enhanced vegetation activity in Eastern Australia over 1998–2012 reversed the original degradation trend before 1998, but vegetation activity in Western Australia degraded after 1998. The inter-annual fluctuation in the NDVI weakened, and vegetation activity tended to be stable in North America, South Africa, southern East Asia, and northern Australia.

The trend of pixels passing the significance test ($P < 0.1$) was counted for 1982–1998 and 1998–2012 for the different

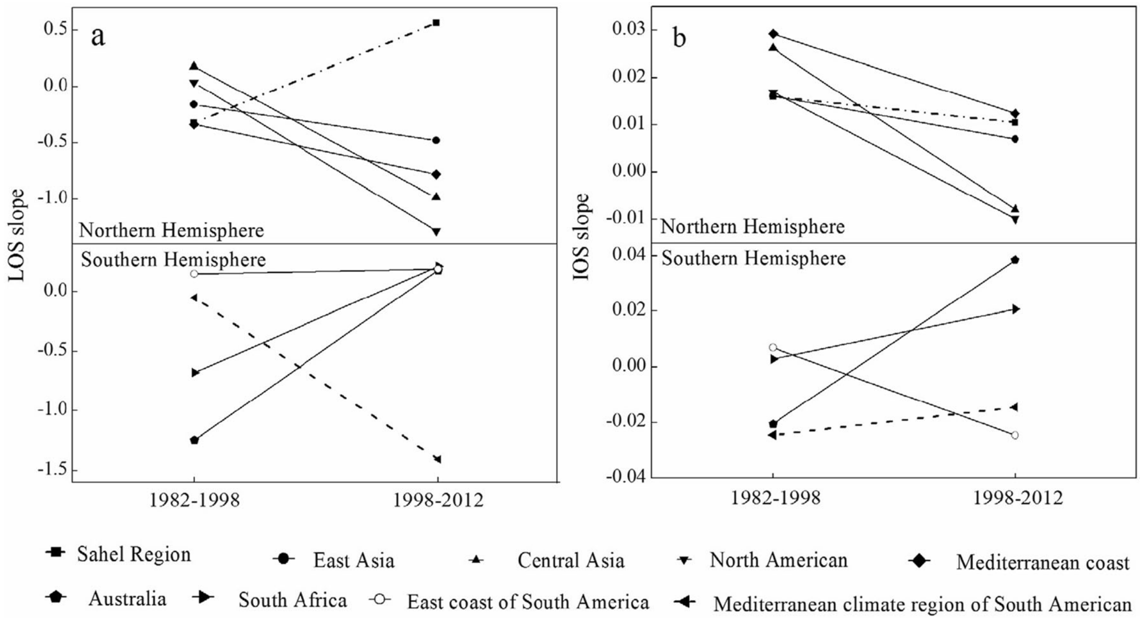


**Fig. 5** The slope of the LOS (**a**) and IOS (**b**) during 1982–1998 and 1998–2012. LOS is the length of growing season, and IOS is the integral of growing season

hemispheres. The results showed that the slope of NDVI was almost positive over 1982–1998, which indicates that the NDVI mainly exhibited an increasing trend, and the variation in the slope was small. This means that the vegetation activity slowly increased over the period (Fig. 7a). The slope of NDVI transformed from a packed first and forth quadrant to a random distribution in four quadrants over 1998–2012 (Fig. 7b). This indicates that the majority of NDVI values began to decrease, and a part of the vegetation activity began to weaken in the global desert/grassland biome transition zones. In contrast, the trend of the fluctuation of vegetation activity exhibited an opposite characteristic (Fig. 8). Both weakening and enhancing fluctuation pixels exist in the Northern and Southern hemispheres over 1982–1998 (Fig. 8a), which means that the fluctuation of vegetation activity in this period is complex. However, the fluctuation values became positive after 1998 (Fig. 8b), meaning that vegetation activity in most areas fluctuated more significantly. From the above results, we deduced that vegetation with poor adaptation to the disturbance of the external environment was more sensitive and fragile. For this

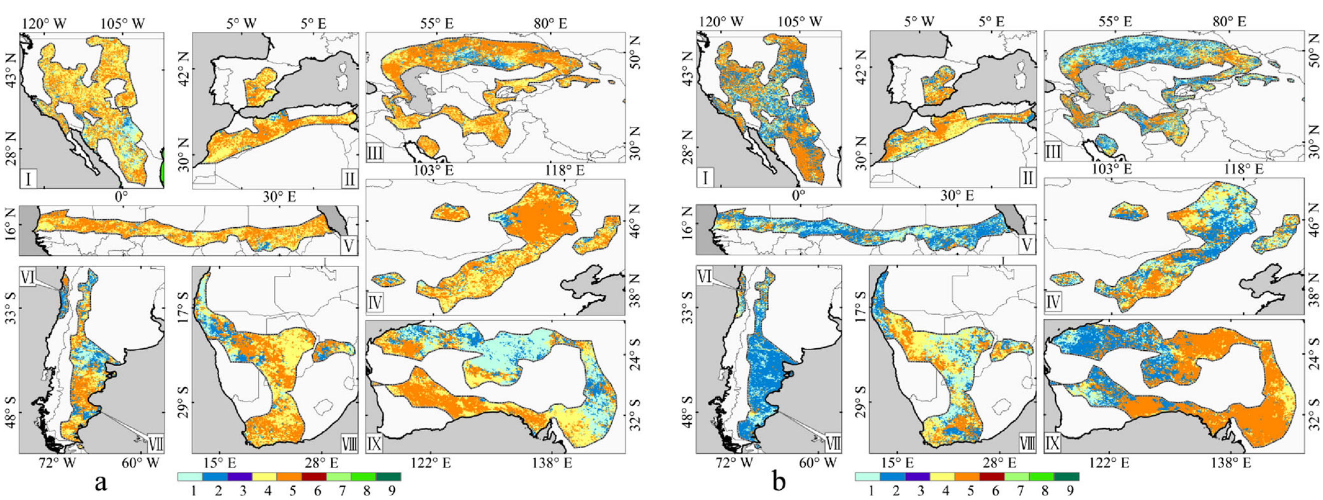


**Fig. 6** Spatial distribution of vegetation activity modes for the period 1982–1998 (**a**) and 1998–2012 (**b**). (1) Decreasing trend and weakening fluctuation, (2) decreasing trend and enhancing fluctuation, (3) decreasing trend and stable fluctuation, (4) increasing trend and weakening fluctuation, (5) increasing trend and enhancing fluctuation, (6) increasing trend and stable fluctuation, (7) no trend and weakening fluctuation, (8) no trend and enhancing fluctuation, and (9) no trend and stable fluctuation. Nine partitions are (I) North American, (II) Mediterranean Coast, (III) Central Asia, (IV) East Asia, (V) Sahel Region, (VI) Mediterranean climate region of South American West Coast, (VII) East Coast of South America, (VIII) South Africa, and (IX) Australia

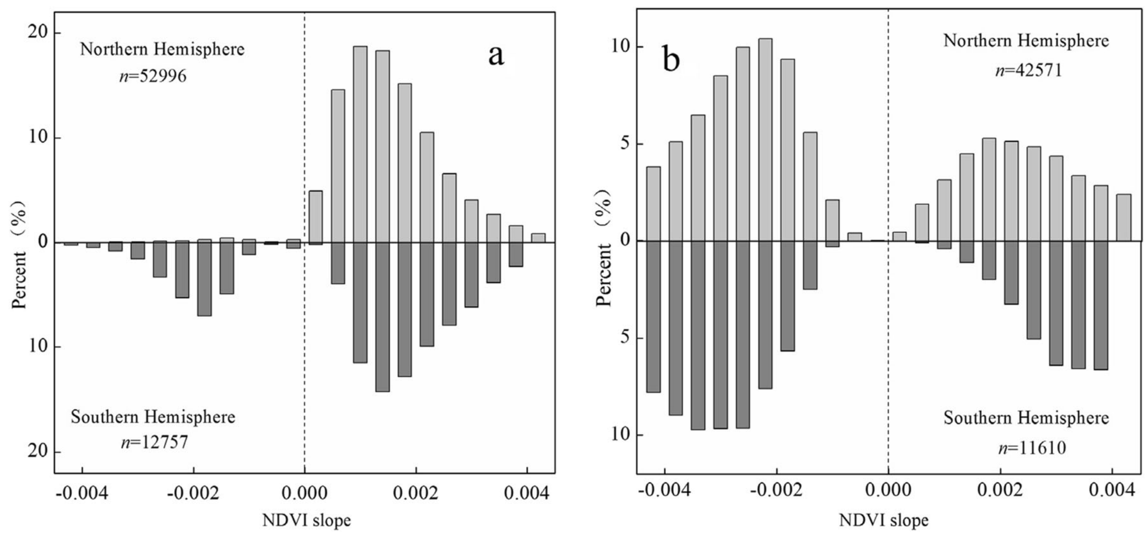


**Fig. 7** Frequency distribution of NDVI slopes for 1982–1998 (**a**) and 1998–2012 (**b**) in different hemispheres

reason, the ecological environment became more unstable, with extreme weather occurring at a higher frequency and climatic events of higher intensity occurring in global desert/grassland biome transition zones.

### 3.3 Relationship between vegetation activity and climatic factors

Climate is the key factor influencing vegetation activity. Long-term average climate determines the distribution pattern and evolution of global vegetation at a large scale, and inter-annual climate change can also cause the inter-annual fluctuation of vegetation. To reveal the response mechanism of vegetation to climate factors in the last 30 years, the tendencies of temperature, precipitation, evapotranspiration, and radiation were calculated for 1982–1998 and 1998–2012 (Table 4). From 1982 to 1998, the climate in most desert/grassland biome transition zones was warming and wetting and precipitation decreased only in North America and the Mediterranean climatic region of South American West Coast. Meanwhile, the evapotranspiration significantly increased, except in North America and South America, and photosynthetically active radiation declined almost everywhere except the Mediterranean Coast. After 1998, the warming trend tended to slow down and even completely reversed in some areas, which was consistent with the IPCC Assessment Report (Stocker et al. 2013). There were obvious differences, whereby precipitation witnessed a considerable increase in Australia, South Africa, and the Mediterranean Coast, and slight increases or decreases in other regions, particularly in South America. Evapotranspiration significantly decreased, and photosynthetically active radiation declined slightly or even increased, particularly in East Asia.

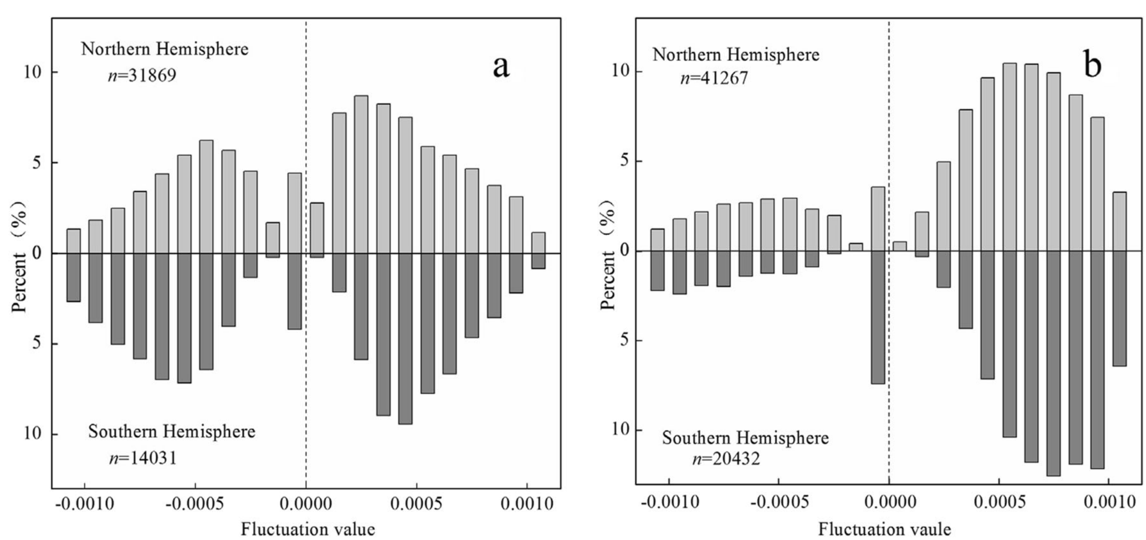


**Fig. 8** Frequency distribution of NDVI fluctuation for 1982–1998 (**a**) and 1998–2012 (**b**) in different hemispheres

**Table 4** Trend of climatic factors in desert/grassland biome transition zones during 1982–1998 and 1998–2012

| | | I. North American | II. Mediterranean Coast | III. Central Asia | IV. East Asia | V. Sahel Region | VI. Mediterranean climate region of South America West Coast | VII. East Coast of South America | VIII. South Africa | IX. Australia |
|---|---|---|---|---|---|---|---|---|---|---|
| 1982–1997 | Temperature (K) | 0.0507 | 0.0335 | 0.0205 | 0.0825 | 0.0312 | 0.0163 | 0.0142 | 0.0115 | 0.0416 |
| | Precipitation (mm/day) | −0.0033 | 0.0061 | 0.0002 | 0.0061 | 0.0153 | −0.0245 | 0.0048 | 0.0069 | 0.0023 |
| | Evapotranspiration (mm/day) | −0.0276 | 0.0137 | 0.0145 | 0.0162 | 0.0231 | −0.0237 | −0.0059 | 0.0185 | 0.0246 |
| | Radiation (W $m^{-2}$ s) | −251 | 49 | −4 | −144 | −60 | −173 | −64 | −18 | −33 |
| 1998–2012 | Temperature (K) | 0.0044 | −0.0314 | −0.0282 | −0.0403 | 0.0404 | 0.1219 | −0.0019 | −0.0328 | −0.0097 |
| | Precipitation (mm/day) | −0.0027 | 0.0166 | −0.0008 | 0.0013 | 0.0051 | −0.0397 | −0.0214 | 0.0070 | 0.0026 |
| | Evapotranspiration (mm/day) | −0.0268 | −0.0004 | −0.0089 | −0.0263 | −0.0146 | −0.0687 | −0.0404 | 0.0014 | −0.0312 |
| | Radiation (W $m^{-2}$ s) | 82 | −46 | 105 | 1013 | −12 | −269 | −102 | 17 | 28 |

To explore the effects of climatic factors on vegetation activity in each desert/grassland biome transition zone, the partial correlations involving NDVI and temperature, precipitation, evapotranspiration, and radiation were determined pixel by pixel (Fig. 9). The results showed that the NDVI was positively correlated to evapotranspiration and precipitation and negatively correlated to radiation. However, there were regional differences in the correlation between the NDVI and temperature, whereby the NDVI and temperature were positively correlated in middle-latitude areas and negatively correlated in low-latitude areas. The number of pixels with a partial correlation coefficient of NDVI and evapotranspiration, precipitation, temperature, and radiation that passed the significance test level ($P < 0.1$) accounts for 36, 29, 28, and 18%, respectively, of the entire desert/grassland biome transition zone. In conclusion, NDVI is positively correlated with evapotranspiration or precipitation at varying levels, which are the most important factors driving vegetation activity in most global desert/grassland biome transition zones.

To further explore the inner relationship between NDVI and climatic factors, the pixels passing the significance test ($P < 0.1$) were counted and the correlation of NDVI slope and climatic factors slope was determined. The scattered points on the slope of the NDVI and the slope of temperature in low-latitude areas are mainly distributed along the second and fourth quadrants (Fig. 10a) with a negative correlation, which means that rising temperature would strongly constrain vegetation activity from 30° N to 30° S. Although rising temperature can promote vegetation growth in middle-latitude areas, the randomly scattered points on the slope of the NDVI and the slope of temperature indicate that no significant correlation was found (Fig. 10b). With a positive correlation for the scattered points of the slope of NDVI and precipitation, evapotranspiration is mainly distributed along the first and third quadrants (Fig. 10c–f). This meant that the variation in precipitation and evapotranspiration could affect changes in NDVI to some extent. The slope of NDVI and the slope of radiation almost did not correlate, especially for the period of 1998–2012 (Fig. 10g–h).

## 4 Discussion

The correlation analysis showed that the annual NDVI of the Mediterranean Coast and the East Coast of South America has a highly significant negative correlation and that vegetation growth on both sides of the Atlantic has a marked "seesaw" phenomenon. This might be due to the variation in the intensity of ocean currents between the South and the North Atlantic. The IPCC Fourth Assessment Report stated that salinity had been decreasing in the northern part of the North Atlantic and that the meridional overturning circulation (MOC) of the Atlantic Ocean would slow down during the

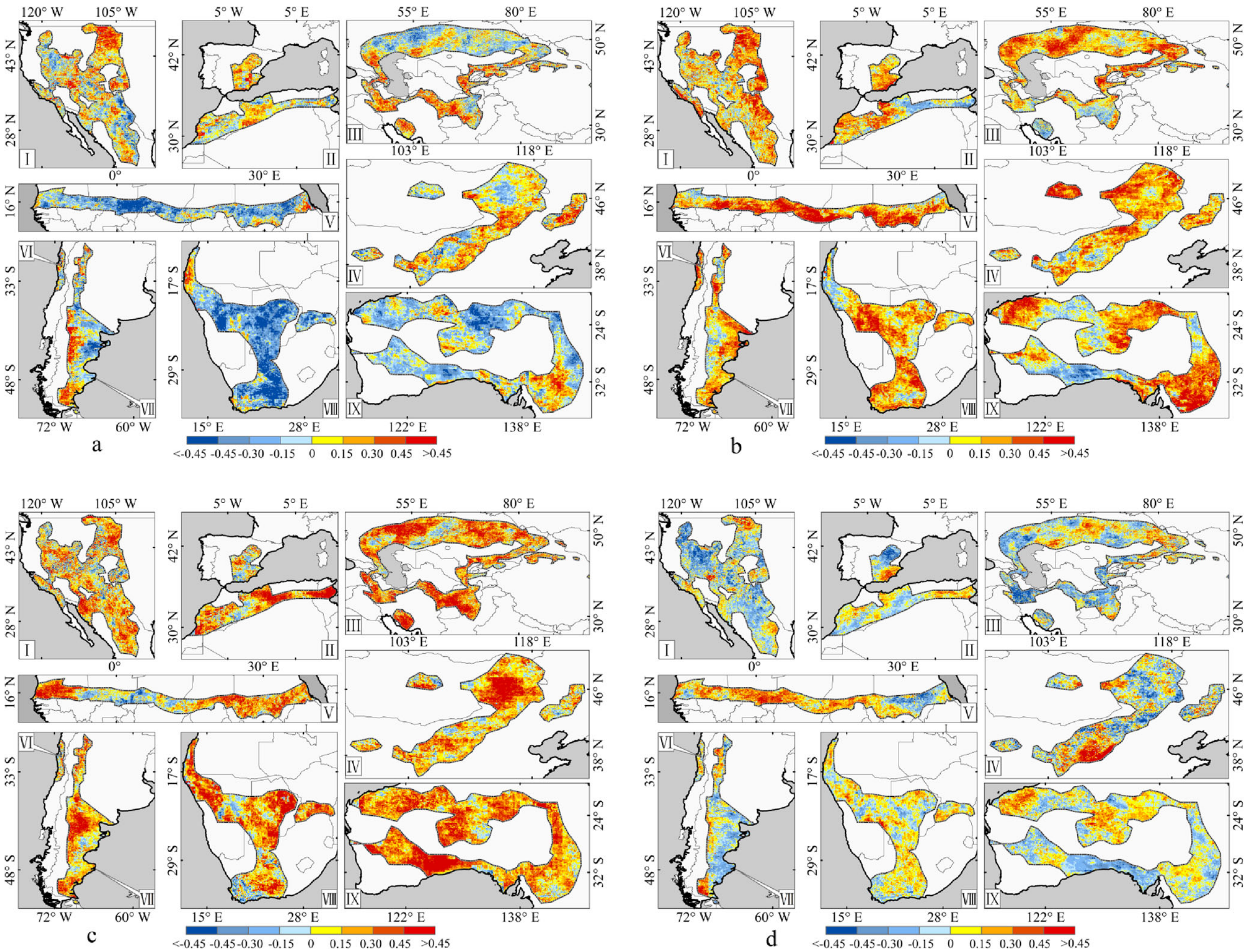


**Fig. 9** Partial correlation coefficient between NDVI and temperature (**a**), precipitation (**b**), evapotranspiration (**c**), and radiation (**d**). Nine partitions are (I) North American, (II) Mediterranean Coast, (III) Central Asia, (IV) East Asia, (V) Sahel Region, (VI) Mediterranean climate region of South American West Coast, (VII) East Coast of South America, (VIII) South Africa, and (IX) Australia

twenty-first century (Parry et al. 2007). With the weakened circulation, the northward North Atlantic Drift might be projected to weaken, and warm seawater to stagnate, in the middle-latitude areas; this would promote increasing precipitation and consequently vegetation growth. Thus, vegetation activity generally increased along the Mediterranean Coast. Moreover, the changes in the warm Brazilian current may have been driven by changes in the ocean currents of the North Atlantic, which led to climatic fluctuations, with precipitation decreases and vegetation degradation along the East Coast of South America. This gave rise to a significant negative correlation between vegetation growth along the Mediterranean Coast and that of the East Coast of South America. Certainly, in order to be established, this hypothesis requires further analysis of changes in the ocean currents.

Previous studies observed that the average NDVI in the global semi-arid regions had increased by 0.015 in 1981–2007 (Fensholt et al. 2012), which agrees with the results of this study. From the NDVI trend, in the last 30 years, the vegetation activity has been enhanced in global desert/grassland biome transition zones. Nevertheless, due to diverse climatic conditions, there are obvious discrepancies in the characteristics of vegetation activity in different periods of time. Over 1982–1998, with a warming and wetting climate, the vegetation growth generally increased with smaller changes in the slope. However, with the change of precipitation pattern in different regions, the vegetation growth changed accordingly and the trend of NDVI was completely reversed in Central Asia, the Sahel, and South America. Vegetation activity was enhanced in Eastern Australia and weakened in Western Australia. The spatial differentiation in vegetation activity increased in East Asia, North America, South Africa, and Australia. Previous studies found the precipitation and NDVI in arid regions has a close relationship but that their slopes did not correlate over 1981–2003 (Helldén and Tottrup 2008). However, this research found that, to some extent, the slope of NDVI is correlated with the slope of precipitation, which may be due to the difference in the time scale.

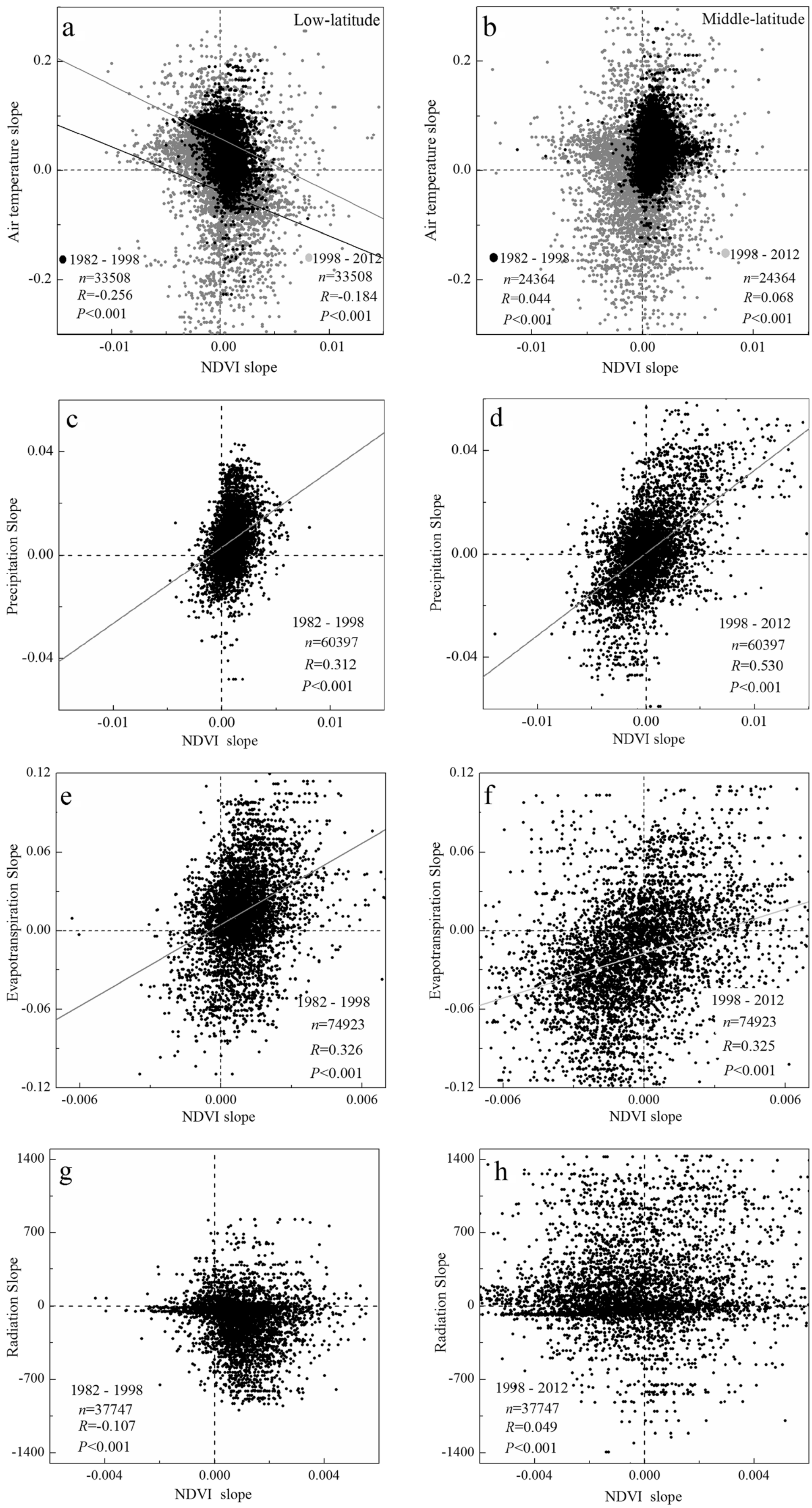
a
Low-latitude
Air temperature slope
NDVI slope
1982 - 1998
n=33508
R=-0.256
P<0.001
1998 - 2012
n=33508
R=-0.184
P<0.001
b
Middle-latitude
Air temperature slope
NDVI slope
1982 - 1998
n=24364
R=0.044
P<0.001
1998 - 2012
n=24364
R=0.068
P<0.001
c
Precipitation Slope
NDVI slope
1982 - 1998
n=60397
R=0.312
P<0.001
d
Precipitation Slope
NDVI slope
1998 - 2012
n=60397
R=0.530
P<0.001
e
Evapotranspiration Slope
NDVI slope
1982 - 1998
n=74923
R=0.326
P<0.001
f
Evapotranspiration Slope
NDVI slope
1998 - 2012
n=74923
R=0.325
P<0.001
g
Radiation Slope
NDVI slope
1982 - 1998
n=37747
R=-0.107
P<0.001
h
Radiation Slope
NDVI slope
1998 - 2012
n=37747
R=0.049
P<0.001

◀ **Fig. 10** Scatter plot of NDVI slope and air temperature slope in low latitude (**a**), air temperature slope in middle latitude (**b**), precipitation slope over 1982–1998 (**c**), precipitation slope over 1998–2012 (**d**), evapotranspiration slope over 1982–1998 (**e**), evapotranspiration slope over 1998–2012 (**f**), radiation slope over 1982–1998 (**g**), and radiation slope over 1998–2012 (**h**)

In addition to the temperature, precipitation, evapotranspiration, and radiation factors that were considered in this study, El Niño, La Niña, and other large-scale climate change events also impact vegetation activity (Leeuwen et al. 2013). Consequently, future studies on the effect of global climate change on vegetation need to further discuss these phenomena. In addition to natural factors, human activities also play a pivotal role in the change of vegetation in the desert/grassland biome transition zone, which is a complex issue that needs to be considered in future research. Furthermore, due to the wide distribution and varying climate types of the global desert/grassland biome transition zones, only the inter-annual variability of vegetation activity was analyzed; the study of intra-annual variations should be further investigated in future work (Jeong et al. 2011; Tateishi and Ebata 2004).

## 5 Conclusions

In this study, the vegetation activity and evolutionary tendencies of the desert/grassland biome transition zones were analyzed based on the GIMMS3g NDVI dataset. Additionally, the relationship between vegetation activity and climatic factors was analyzed. The following conclusions are obtained:

At the same latitude of the same hemisphere, vegetation activity in most of the desert/grassland biome transition zones showed a positive correlation and identical change trends. However, the vegetation activity on both sides of the Atlantic showed a marked “seesaw” phenomenon, which may be the result of global climate evolution.

The LOS and the IOS of desert/grassland biome transition zones recorded striking differences of phenology in the Northern and Southern hemispheres during the two time periods. In the Northern Hemisphere, the slopes of LOS and IOS for 1998–2012 are much lower than they were for 1982–1998, which indicates that vegetation activity weakened after 1998. However, the opposite trend occurred in the Southern Hemisphere, where vegetation activity was enhanced after 1998 except for South America.

In 1998, the mode of vegetation activity in the desert/grassland biome transition zones altered significantly. Over 1982–1998, most areas showed vegetation activity increasing and enhancing fluctuation. However, the trend and fluctuation changed approximately after 1998 and exhibited an intense spatial differentiation. Based on these results, it can be inferred that the ecosystem of the desert/grassland biome transition zones became more sensitive and fragile in the twenty-first century.

Climate is the key factor for vegetation activity in the global desert/grassland biome transition zones. Precipitation and evapotranspiration significantly affected vegetation activity. Moreover, the rising temperature restricted the vegetation activity in low-latitude areas and promoted it in middle-latitude areas.

**Acknowledgements** We are grateful to the anonymous reviewers for their comments on earlier versions of the manuscript.

**Funding information** The present study was sponsored by the National Science Foundation of China (No. 41661003), Natural Science Foundation of Ningxia Province (No. NX16010), First Class Disciplines Program in Western China of Ningxia Province (Ecology, No. NXYLXK2017B06), and “Light of West China” Program of the Chinese Academy of Sciences (No. XAB2017AW01).

## Compliance with ethical standards

**Conflict of interest** The authors declare that they have no conflict of interest.

## References

Anyamba A, Small J, Tucker C, Pak E (2014) Thirty-two years of Sahelian zone growing season non-stationary NDVI3g patterns and trends. Remote Sens 6(4):3101–3122

Bao G, Bao Y, Sanjjava A, Qin Z, Zhou Y, Xu G (2015) NDVI-indicated long-term vegetation dynamics in Mongolia and their response to climate change at biome scale. Int J Climatol 35(14):4293–4306

Bao G, Bao Y, Qin Z et al (2016) Modeling net primary productivity of terrestrial ecosystems in the semi-arid climate of the Mongolian Plateau using LSWI-based CASA ecosystem model. Int J Appl Earth Obs Geoinf 46:84–93

Beck HE, McVicar TR, Dijk AIJM, Schellekens J, Jeu RAM, Bruijnzeel LA (2011) Global evaluation of four AVHRR–NDVI data sets: intercomparison and assessment against Landsat imagery. Remote Sens Environ 115(10):2547–2563

Bunn AG, Goetz SJ, Kimball JS, Zhang K (2007) Northern high-latitude ecosystems respond to climate change. Eos Trans Am Geophys Union 88(34):333–335

Campo-Bescós M, Muñoz-Carpena R, Southworth J, Zhu L, Waylen P, Bunting E (2013) Combined spatial and temporal effects of environmental controls on long-term monthly NDVI in the southern Africa savanna. Remote Sens 5(12):6513–6538

Chen M, Xie P, Janowiak JE, Arkin PA (1997) Global land precipitation: a 50-yr monthly analysis based on gauge observations. Bull Amer Meteorol Soc 78(11):2539–2558

Chen Y, Sun Z, Qin Z, Propastin P, Wang W, Li J, Ruan H (2017a) Modeling the regional grazing impact on vegetation carbon sequestration ability in Temperate Eurasian Steppe. J Integr Agric 16(10): 2323–2336

Chen Y, Li J, Ju W et al (2017b) Quantitative assessments of water-use efficiency in Temperate Eurasian Steppe along an aridity gradient. PLoS ONE 12(7):e0179875. https://doi.org/10.1371/journal.pone.0179875

Dee DP, Uppala SM, Simmons AJ et al (2011) The ERA-Interim reanalysis: configuration and performance of the data assimilation system. Q J R Meteorol Soc 137(656):553–597

Du L, Tian Q, Yu T, Meng Q, Jancso T, Udvardy P, Huang Y (2013) A comprehensive drought monitoring method integrating MODIS and TRMM data. Int J Appl Earth Obs Geoinf 23:245–253

Du L, Song N, Liu K et al (2017) Comparison of two simulation methods of the Temperature Vegetation Dryness Index (TVDI) for drought monitoring in semi-arid regions of China. Remote Sens 9(2):177. https://doi.org/10.3390/rs9020177

Ebita A, Kobayashi S, Ota Y et al (2011) The Japanese 55-year reanalysis "JRA-55": an interim report. SOLA 7(1):149–152

Fan Y, Dool H (2008) A global monthly land surface air temperature analysis for 1948-present. J Geophys Res-Atmos 113(D1):18. https://doi.org/10.1029/2007jd008470

Fensholt R, Langanke T, Rasmussen K et al (2012) Greenness in semi-arid areas across the globe 1981–2007: an earth observing satellite based analysis of trends and drivers. Remote Sens Environ 121(2): 144–158

Forkel M, Carvalhais N, Verbesselt J, Mahecha M, Neigh C, Reichstein M (2013) Trend change detection in NDVI time series: effects of inter-annual variability and methodology. Remote Sens 5(5):2113–2144

Helldén U, Tottrup C (2008) Regional desertification: a global synthesis. Glob Planet Change 64(3):169–176

Hochstrasser T, Kröel-Dulay G, Peters DPC, Gosz JR (2002) Vegetation and climate characteristics of arid and semi-arid grasslands in North America and their biome transition zone. J Arid Environ 51(1):55–78

Huang Y, Tian Q, Du L, Sun S (2013) Analysis of spatial-temporal variation of agricultural drought and its response to ENSO over the past 30 years in the Huang-Huai-Hai region. Terr Atmos Ocean Sci 24(4):745–7591

Jeganathan C, Dash J, Atkinson PM (2014) Remotely sensed trends in the phenology of northern high latitude terrestrial vegetation, controlling for land cover change and vegetation type. Remote Sens Environ 143(5):154–170

Jeong SJ, Chang-Hoi HO, Gim HJ, Brown ME (2011) Phenology shifts at start vs. end of growing season in temperate vegetation over the Northern Hemisphere for the period 1982–2008. Glob Change Biol 17(7):2385–2399

Jönsson P, Eklundh L (2004) TIMESAT: a program for analyzing time-series of satellite sensor data. Comput Geosci 30(8):833–845

Karl TR, Arguez A, Huang B et al (2015) Possible artifacts of data biases in the recent global surface warming hiatus. Science 348(6242): 1469–1472

Kobayashi S, Ota Y, Harada Y et al (2015) The JRA-55 reanalysis: general specifications and basic characteristics. J Meteorol Soc Jpn 93(1):5–48

Kröel-Dulay G, Ódor P, Peters DPC, Hochstrasser T (2004) Distribution of plant species at a biome transition zone in New Mexico. J Veg Sci 15(4):531–538

Laloyaux P, Balmaseda M, Dee D, Mogensen K, Janssen P (2016) A coupled data assimilation system for climate reanalysis. Q J R Meteorol Soc 142(694):65–78

Leeuwen WJD, Hartfield K, Miranda M, Meza FJ (2013) Trends and ENSO/AAO driven variability in NDVI derived productivity and phenology alongside the Andes mountains. Remote Sens 5(3): 1177–1203

Martínez B, Gilabert MA (2009) Vegetation dynamics from NDVI time series analysis using the wavelet transform. Remote Sens Environ 113(9):1823–1842

Meehl GA, Teng H, Arblaster JM (2014) Climate model simulations of the observed early-2000s hiatus of global warming. Nat Clim Chang 4:898–902

Myneni RB, Keeling C, Tucker C, Asrar G, Nemani R (1997) Increased plant growth in the northern high latitudes from 1981 to 1991. Nature 386(6626):698–702

Parry ML, Canziani OF, Palutikof JP, Linden PJ, Hanson CE (2007) Climate change 2007: impacts, adaptation and vulnerability. Cambridge University Press, Cambridge, p 976

Pinzon J, Tucker C (2014) A non-stationary 1981–2012 AVHRR NDVI3g time series. Remote Sens 6(8):6929–6960

Qian S, Fu Y, Pan F (2010) Climate change tendency and grassland vegetation response during the growth season in Three-River Source Region. Sci China-Earth Sci 53(10):1506–1512

Ren J (2008) Classification and cluster applicable for grassland type. Acta Agrestia Sinica 16(1):4–10

Rogier DJ, Sytze DB, Allard DW, Schaepman ME, Dent DL (2011) Analysis of monotonic greening and browning trends from global NDVI time-series. Remote Sens Environ 115(2):692–702

Scholze M, Knorr W, Arnell NW, Prentice IC (2006) A climate-change risk analysis for world ecosystems. Proc Natl Acad Sci U S A 103(35):13116–13120

Shi P, Sun S, Wang M et al (2014) Climate change regionalization in China (1961–2010). Sci China-Earth Sci 57(11):2676–2689

Slayback DA, Pinzon JE, Los SO, Tucker CJ (2010) Northern hemisphere photosynthetic trends 1982–99. Glob Change Biol 9(1):1–15

Stocker TF, Qin D, Plattner GK et al (2013) Climate change 2013: the physical science basis. Cambridge University Press, Cambridge, p 1535

Tateishi R, Ebata M (2004) Analysis of phenological change patterns using 1982–2000 Advanced Very High Resolution Radiometer (AVHRR) data. Int J Remote Sens 25(12):2287–2300

Tchuenté ATK, Roujean JL, Jong SMD (2011) Comparison and relative quality assessment of the GLC2000, GLOBCOVER, MODIS and ECOCLIMAP land cover data sets at the African continental scale. Int J Appl Earth Obs Geoinf 13(2):207–219

Trenberth KE (2015) Has there been a hiatus? Science 349(6249):691–692

Trenberth KE, Fasullo JT (2013) An apparent hiatus in global warming? Earth Future 1(1):19–32

Uppala SM, Kållberg PW, Simmons AJ et al (2005) The ERA-40 re-analysis. Q J R Meteorol Soc 131(612):2961–3012

Weiss JL, Gutzler DS, Coonrod JEA, Dahm CN (2004) Seasonal and inter-annual relationships between vegetation and climate in central New Mexico, USA. J Arid Environ 57:507–534

Zeng F, Collatz G, Pinzon J, Ivanoff A (2013) Evaluating and quantifying the climate-driven interannual variability in Global Inventory Modeling and Mapping Studies (GIMMS) Normalized Difference Vegetation Index (NDVI3g) at global scales. Remote Sens 5(8): 3918–3950